

# Nuclear structure of $97\text{Y}$ in the interacting boson fermion plus broken pair model and the nature of the 3.523 MeV high-spin isomer

---

Lhersonneau, G.; Brant, Slobodan; Paar, Vladimir; Vretenar, Dario

Source / Izvornik: **Physical Review C - Nuclear Physics, 1998, 57, 681 - 687**

Journal article, Published version

Rad u časopisu, Objavljena verzija rada (izdavačev PDF)

<https://doi.org/10.1103/PhysRevC.57.681>

Permanent link / Trajna poveznica: <https://um.nsk.hr/um:nbn:hr:217:279476>

Rights / Prava: [In copyright](#) / [Zaštićeno autorskim pravom.](#)

Download date / Datum preuzimanja: **2025-01-25**



Repository / Repozitorij:

[Repository of the Faculty of Science - University of Zagreb](#)



# Nuclear structure of $^{97}\text{Y}$ in the interacting boson fermion plus broken pair model and the nature of the 3.523 MeV high-spin isomer

G. Lhersonneau

*Department of Physics, University of Jyväskylä, P.O. Box 35, FIN-40351, Jyväskylä, Finland*

S. Brant, V. Paar, and D. Vretenar

*Department of Physics, Faculty of Science, University of Zagreb, Zagreb, Croatia*

(Received 26 June 1997)

Nuclear structure of  $^{97}\text{Y}$  is described in the interacting boson fermion plus broken pair model, including quasiproton and quasiproton-two-quasineutron configurations in the basis states. In particular, the yrast bands and the decay of the  $27/2^-$  high-spin isomer are accounted for in this approach. [S0556-2813(98)04102-8]

PACS number(s): 27.60.+j, 21.10.Pc, 21.10.Re, 21.60.Fw

## I. INTRODUCTION

The region of neutron-rich nuclei immediately beyond the  $N=56$  subshell closure is of particular interest for nuclear structure studies because of a very rapid phase transition from spherical to strongly deformed shape and the coexistence of these shapes for  $N=58-60$  nuclei [1]. The  $^{96}\text{Zr}$  nucleus with the  $Z=40$  and  $N=56$  closed subshells exhibits a shell-model type of structure [2]. On the other hand, already the  $^{99}\text{Y}_{60}$  nucleus has properties of a symmetric rotor [3], while the  $^{98}\text{Y}_{59}$  odd-odd nucleus contains an excited rotational band which coexists with spherical states [4]. The  $^{97}\text{Y}_{58}$  nucleus with one proton hole and two neutron particles beyond  $^{96}\text{Zr}$  exhibits a family of levels associated with the  $\pi g_{9/2}$  proton configuration [5-7].

Positive-parity states of  $^{97}\text{Y}$  have been previously studied theoretically in the framework of the interacting boson fermion model (IBFM) [8]. In this way, only the states associated with coupling of a particle-type quasiparticle  $\pi \tilde{g}_{9/2}$  to the  $\text{SU}(5)$  boson core were described, but it was not possible to describe the states based on three-quasiparticle configurations. In this paper, we describe both the positive and negative parity states in  $^{97}\text{Y}$  employing the extension of the interacting boson fermion model by including also the broken pairs of neutrons. This extended model is referred to as the interacting boson fermion plus broken pair model (IBFBPM) [9-11]. In this way, both the one- and three-quasiparticle states coupled to the  $\text{SU}(5)$  boson core are included and mixing between them is accounted for. Particular attention is given to description of the 3.523 MeV isomer which was previously assigned as the  $[\pi \tilde{g}_{9/2}, (\nu \tilde{g}_{7/2}, \nu \tilde{h}_{11/2}) 9] 27/2^-$  three-quasiparticle configuration [6].

## II. CALCULATION FOR $^{97}\text{Y}$ IN THE INTERACTING BOSON FERMION PLUS BROKEN PAIR MODEL (IBFBPM)

The interacting boson model (IBM) of Iachello and Arima [12,13], the interacting boson fermion model (IBFM) [14-16] and the interacting boson fermion fermion model (IBFFM) [17,18] provide a useful framework for description of nuclear structure in even-even, odd-even, and odd-odd

nuclei, respectively. In descriptions of the high-spin states in even-even nuclei, the IBM framework was further extended by including broken pairs in addition to the interacting  $s$  and  $d$  bosons [19-22]. Analogously, the IBFM for odd-even nuclei has been extended by adding one broken pair [9,10]. This model will be referred to as IBFBPM. The IBFBPM configuration space of an odd-even nucleus with  $2N+1$  valence nucleons comprises

$$|N \text{ bosons} \otimes 1 \text{ fermion}\rangle + |(N-1) \text{ bosons} \otimes 1 \text{ broken pair} \otimes 1 \text{ fermion}\rangle. \quad (2.1)$$

The IBFBPM Hamiltonian includes four terms: the interacting boson model (IBM) Hamiltonian [12], the boson-fermion interactions of the interacting boson-fermion model [14], the fermion Hamiltonian, and a pair breaking interaction that mixes one-fermion and three-fermion states. The definition of parameters in the IBM and IBFM terms in this article is taken according to Ref. [23]. For the last term, a simple interaction was employed [9]:

$$V_{\text{mix}} = -U_0 \left\{ \sum_{j_1 j_2} u_{j_1} u_{j_2} (u_{j_1} v_{j_2} + u_{j_2} v_{j_1}) \times \langle j_1 \| Y_2 \| j_2 \rangle^2 \frac{1}{\sqrt{2j_2+1}} ([a_{j_2}^\dagger \times a_{j_2}^\dagger]_0 \cdot s) + \text{H.c.} \right\} - U_2 \left\{ \sum_{j_1 j_2} (u_{j_1} v_{j_2} + u_{j_2} v_{j_1}) \langle j_1 \| Y_2 \| j_2 \rangle \times ([a_{j_1}^\dagger \times a_{j_2}^\dagger]_2 \cdot \tilde{d}) + \text{H.c.} \right\}. \quad (2.2)$$

In the IBFBPM calculation for  $^{97}\text{Y}$  we account for broken neutron pairs, i.e., one-quasiproton-two-quasineutron states are included in the basis states (2.1). Thus, there are two boson-fermion and two fermion-fermion interaction terms contributing to the corresponding matrix elements. We employ as core the spherical nucleus  $^{96}\text{Sr}_{58}$ . This nucleus was used as the  $\text{SU}(5)$  IBM core in the previous IBFM calculation for  $^{97}\text{Y}$  [8] and in the IBFFM calculation for  $^{98}\text{Y}$  [24]. We use here the same IBM parametrization:  $h_1=0.815$

MeV,  $h_2=h_3=h_{40}=0$  MeV,  $h_{42}=-0.37$  MeV,  $h_{44}=0.22$  MeV, with the boson number  $N=4$ .

In the calculation for the positive-parity states the  $\pi\tilde{g}_{9/2}$  and  $\pi\tilde{d}_{5/2}$  proton quasiparticle states are included with quasiparticle energies 2.0 and 8.0 MeV, and occupation probabilities 0.044 and 0.01, respectively. In order to keep the size of configuration space manageable (the maximum dimension of the configuration space is 1600), the low-spin negative parity quasiproton states  $\pi\tilde{p}_{1/2}$ ,  $\pi\tilde{p}_{3/2}$ ,  $\pi\tilde{f}_{5/2}$ , have been omitted from the calculation. In fact, these configurations give very small contributions to the high-spin states considered here and this approximation has a very small effect. In the previous IBFM calculation only the  $\pi\tilde{g}_{9/2}$  positive parity proton quasiparticle was included. Here the  $\pi\tilde{d}_{5/2}$  quasiparticle from the next major shell is also included since it plays an important role in generating the  $\Delta J = 1$  pattern for the positive-parity yrast band. A sizable influence of the inclusion of  $\pi\tilde{d}_{5/2}$  configuration is due to the large non-spinflip matrix element  $\langle\pi d_{5/2}\|Y_2\|\pi g_{9/2}\rangle$ . Without inclusion of the  $\pi\tilde{d}_{5/2}$  configuration we would obtain a decoupled yrast band pattern. The occupation probability of the  $\pi\tilde{g}_{9/2}$  quasiparticle state is taken from Ref. [8] and the  $\pi\tilde{d}_{5/2}$  state, lying above the valence shell, is of a particle character, with a very small occupation probability. The  $\nu\tilde{s}_{1/2}$ ,  $\nu\tilde{g}_{7/2}$ ,  $\nu\tilde{h}_{11/2}$ , and  $\nu\tilde{d}_{5/2}$  neutron quasiparticle states are taken with quasiparticle energies 1.42, 1.65, 1.94, and 2.04 MeV, and occupation probabilities 0.17, 0.12, 0.08, and 0.93, respectively. The neutron quasiparticles have been deduced from the BCS calculation starting from the Kisslinger-Sorensen parametrization [25], with an enlarged gap between the  $\nu d_{5/2}$  and the other valence shell single-particle states. The highest-lying quasiparticle state,  $\nu\tilde{d}_{3/2}$ , was omitted from the IBFBPM configuration space, since it has only a minor influence on the levels which are investigated here.

The boson-fermion interaction strengths for neutrons are  $\Gamma_0^\nu=0.8$  MeV,  $\Lambda_0^\nu=A_0^\nu=0$  MeV,  $\chi^\nu=-1.0$ , which is similar to the values used in the previous IBFFM calculation for  $^{94}\text{Rb}$  [26]. For protons we take  $\Gamma_0^\pi=0.4$  MeV,  $\Lambda_0^\pi=2.5$  MeV,  $A_0^\pi=0.02$  MeV. The value of  $\Gamma_0^\pi$  is the same as used in the previous IBFM calculation for  $^{97}\text{Y}$  [8], while the value of  $\Lambda_0^\pi$  is somewhat reduced. However, the crucial difference is in the choice of the parameter  $\chi^\pi$  which is  $\chi^\pi=0$ . We have found that only by including the  $\pi\tilde{d}_{5/2}$  fermion and having  $\chi^\pi=0$  makes it possible to obtain in the calculation the normal ordering for positive parity band pattern on the yrast line, i.e.,  $\Delta J=1:9/2_1^+, 11/2_1^+, 13/2_1^+, 15/2_1^+, 17/2_1^+, \dots$ . Otherwise, we would obtain the ordering associated with decoupled band pattern:  $9/2_1^+, 13/2_1^+, 11/2_1^+, 17/2_1^+, 15/2_1^+, \dots$ .

The values of the pair breaking interaction strengths  $U_0, U_2$  and the surface delta interaction strength for neutrons  $V_\delta$  are taken in a qualitative accordance with previous IBFBPM calculations [27,28]:  $U_0=0$  MeV,  $U_2=0.34$  MeV, and  $V_\delta=-0.15$  MeV.

On the other hand, in the calculation of negative-parity states the parametrization is the same as above for the positive-parity states, except for extension of the negative-parity quasiparticle space by including the  $\pi\tilde{p}_{1/2}$ ,  $\pi\tilde{p}_{3/2}$ , and

$\pi\tilde{f}_{5/2}$  quasiparticles with quasiparticle energies 0.73, 1.51, and 1.88 MeV, and occupation probabilities 0.617, 0.924, and 0.929, respectively. These values are close to the BCS solutions corresponding to the Kisslinger-Sorensen parametrization [25]. Furthermore, we increase the magnitude of  $A_0^\pi$  to  $-0.12$  MeV. The  $\pi\tilde{d}_{5/2}$  quasiparticle was omitted from the configuration space for negative-parity states, since its influence is negligible.

The IBFBPM Hamiltonian is diagonalized in the basis (2.1) and we obtain the energy spectra and the wave functions:

$$|J_k^\pi\rangle = \sum_{jn_d\nu R} \xi_{j,n_d\nu R;J} |\pi\tilde{j}, n_d\nu R; J\rangle + \sum_{jj'j''I_{\nu\nu}I_{\pi\nu\nu}, n_d\nu R; J} \eta_{jj'j''I_{\nu\nu}I_{\pi\nu\nu}, n_d\nu R; J} |\pi\tilde{j}, (\nu\tilde{j}', \nu\tilde{j}'')I_{\nu\nu}\rangle |I_{\pi\nu\nu}, n_d\nu R; J\rangle. \quad (2.3)$$

Here  $\pi\tilde{j}$  stands for a proton quasiparticle, and  $\nu\tilde{j}', \nu\tilde{j}''$  for neutron quasiparticles which are coupled to the angular momentum  $I_{\nu\nu}$ . Angular momenta  $j$  and  $I_{\nu\nu}$  are coupled to the three-quasiparticle angular momentum denoted by  $I_{\pi\nu\nu}$ . In the boson part of the wave function, the  $n_d$   $d$ -bosons are coupled to the total boson angular momentum  $R$ . The additional quantum number  $\nu$  is used to distinguish between the  $n_d$ -boson states having the same angular momentum  $R$ . We note that the number of  $s$  bosons associated with the boson state  $|n_d\nu R\rangle$  is  $n_s=N-n_d$ , where  $N$  is the total number of bosons.

In Fig. 1 we present the calculated energy spectrum of  $^{97}\text{Y}$  in comparison to the available data and Table I displays wave functions (2.3) for some states. Figure 2 displays the total weight of components containing three-quasiparticle components

$$P_3(J_k^\pi) = \sum_{jj'j''I_{\nu\nu}I_{\pi\nu\nu}, n_d\nu R} |\eta_{jj'j''I_{\nu\nu}I_{\pi\nu\nu}, n_d\nu R; J}^\pi|^2 \quad (2.4)$$

in the wave functions of yrast and yrare positive- and negative-parity states.

Using the IBFBPM wave functions we calculate the  $E2$  and  $M1$  electromagnetic properties. The effective charges and the fermion gyromagnetic ratios are taken from the previous IBFFM calculation for  $^{94}\text{Rb}$  [26]:  $e^\pi=1.5$ ,  $e^\nu=0.5$ ,  $e^{vib}=2.2$ ,  $\chi=0$ ,  $g_l^\pi=1$ ,  $g_l^\nu=0$ ,  $g_s^\pi=0.7g_s^{\pi,free}=3.910$ ,  $g_s^\nu=0.7g_s^{\nu,free}=-2.678$  and the boson gyromagnetic ratio is  $g_R=Z/A=0.402$ . The calculated  $E2$  and  $M1$  transitions for the positive-parity yrast band are shown in Table II.

It should be noted that in the early applications of IBFM systematic studies were made of an entire range of isotopes in some mass regions, leading to systematics of model parameters [16]. This has helped to show that the parameters are physically meaningful, and to reduce the probability that parameters are forced to reproduce a certain feature in one particular nucleus only. An analog question may be raised in the IBFBPM model calculations. In this sense we have performed a preliminary IBFBPM calculation for  $^{99}\text{Nb}$  in comparison to the present calculation for  $^{97}\text{Y}$ , comparing the

TABLE I. Main components ( $\geq 1\%$ ) in the wave functions of the form given by Eq. (2.3) for some low-lying and yrast states in  $^{97}\text{Y}$ . The boson quantum number  $\nu$  is not needed for components  $\geq 1\%$  and therefore is omitted.

$J_k^\pi$	$\pi \tilde{f}$ or $[\pi \tilde{f}, (\nu \tilde{f}', \nu \tilde{f}'') I_{\nu\nu}] I_{\pi\nu\nu}$	$n_d$	$R$	$\xi$	$J_k^\pi$	$\pi \tilde{f}$ or $[\pi \tilde{f}, (\nu \tilde{f}', \nu \tilde{f}'') I_{\nu\nu}] I_{\pi\nu\nu}$	$n_d$	$R$	$\xi$
$1/2_1^-$	$\pi p_{1/2}$	0	0	0.97		$\pi g_{9/2}$	2	2	0.39
	$\pi p_{3/2}$	1	2	-0.17		$\pi g_{9/2}$	2	4	-0.31
	$\pi f_{5/2}$	1	2	-0.15		$\pi g_{9/2}$	3	4	-0.13
$3/2_1^-$	$\pi p_{1/2}$	1	2	0.25		$[\pi g_{9/2}, (\nu s_{1/2}, \nu d_{5/2}) 2] 9/2$	1	2	-0.10
	$\pi p_{3/2}$	0	0	0.93		$[\pi g_{9/2}, (\nu s_{1/2}, \nu d_{5/2}) 2] 11/2$	0	0	0.17
	$\pi p_{3/2}$	1	2	0.23	$13/2_1^+$	$\pi g_{9/2}$	1	2	-0.84
$5/2_1^-$	$\pi p_{1/2}$	1	2	0.52		$\pi g_{9/2}$	2	2	0.32
	$\pi p_{3/2}$	1	2	-0.11		$\pi g_{9/2}$	2	4	0.31
	$\pi p_{3/2}$	2	4	-0.11		$\pi g_{9/2}$	3	3	-0.10
	$\pi f_{5/2}$	0	0	-0.81		$[\pi g_{9/2}, (\nu s_{1/2}, \nu d_{5/2}) 2] 13/2$	0	0	-0.13
	$[\pi p_{1/2}, (\nu s_{1/2}, \nu d_{5/2}) 2] 5/2$	0	0	0.11	$15/2_1^+$	$\pi g_{9/2}$	2	4	0.73
$7/2_1^-$	$\pi p_{3/2}$	1	2	-0.45		$\pi g_{9/2}$	3	3	-0.50
	$\pi p_{3/2}$	2	4	-0.28		$\pi g_{9/2}$	3	4	0.15
	$\pi f_{5/2}$	1	2	-0.79		$\pi g_{9/2}$	3	6	-0.20
	$\pi f_{5/2}$	2	4	-0.17		$\pi g_{9/2}$	4	4	0.13
	$[\pi f_{5/2}, (\nu s_{1/2}, \nu d_{5/2}) 2] 7/2$	0	0	-0.13		$[\pi g_{9/2}, (\nu s_{1/2}, \nu d_{5/2}) 2] 11/2$	1	2	0.17
$9/2_1^-$	$\pi p_{1/2}$	2	4	0.49		$[\pi g_{9/2}, (\nu s_{1/2}, \nu d_{5/2}) 2] 13/2$	2	2	0.11
	$\pi p_{3/2}$	2	4	0.69		$[\pi g_{9/2}, (\nu g_{7/2})^2 2] 11/2$	1	2	-0.10
	$\pi p_{3/2}$	3	4	-0.13	$17/2_1^+$	$\pi g_{9/2}$	2	4	-0.84
	$\pi f_{5/2}$	1	2	0.11		$\pi g_{9/2}$	3	4	0.34
	$\pi f_{5/2}$	2	2	-0.24		$\pi g_{9/2}$	3	6	0.22
	$\pi f_{5/2}$	2	4	0.27		$[\pi g_{9/2}, (\nu s_{1/2}, \nu d_{5/2}) 2] 13/2$	1	2	-0.19
	$\pi f_{5/2}$	3	4	-0.12		$[\pi g_{9/2}, (\nu g_{7/2})^2 2] 13/2$	1	2	0.14
	$[\pi p_{1/2}, (\nu s_{1/2}, \nu d_{5/2}) 2] 5/2$	1	2	0.12		$[\pi g_{9/2}, (\nu h_{11/2})^2 2] 13/2$	1	2	0.12
	$[\pi p_{3/2}, (\nu s_{1/2}, \nu d_{5/2}) 2] 5/2$	1	2	0.12	$19/2_1^+$	$[\pi g_{9/2}, (\nu d_{5/2}, \nu g_{7/2}) 3] 15/2$	1	2	0.16
	$[\pi p_{1/2}, (\nu d_{5/2}, \nu g_{7/2}) 3] 7/2$	1	2	-0.12		$[\pi g_{9/2}, (\nu d_{5/2}, \nu g_{7/2}) 3] 15/2$	2	2	-0.12
$11/2_1^-$	$[\pi p_{1/2}, (\nu d_{5/2}, \nu g_{7/2}) 4] 9/2$	1	2	-0.35		$[\pi g_{9/2}, (\nu d_{5/2}, \nu g_{7/2}) 4] 15/2$	1	2	-0.24
	$[\pi p_{1/2}, (\nu d_{5/2}, \nu g_{7/2}) 5] 11/2$	0	0	-0.74		$[\pi g_{9/2}, (\nu d_{5/2}, \nu g_{7/2}) 4] 15/2$	2	2	0.15
	$[\pi p_{1/2}, (\nu d_{5/2}, \nu g_{7/2}) 5] 11/2$	2	0	-0.12		$[\pi g_{9/2}, (\nu d_{5/2}, \nu g_{7/2}) 4] 17/2$	1	2	0.30
	$[\pi p_{1/2}, (\nu d_{5/2}, \nu g_{7/2}) 6] 13/2$	1	2	0.32		$[\pi g_{9/2}, (\nu d_{5/2}, \nu g_{7/2}) 4] 17/2$	2	4	-0.15
	$[\pi p_{3/2}, (\nu d_{5/2}, \nu g_{7/2}) 5] 9/2$	1	2	0.12		$[\pi g_{9/2}, (\nu d_{5/2}, \nu g_{7/2}) 5] 17/2$	1	2	-0.22
	$[\pi p_{3/2}, (\nu d_{5/2}, \nu g_{7/2}) 5] 13/2$	1	2	0.11		$[\pi g_{9/2}, (\nu d_{5/2}, \nu g_{7/2}) 5] 17/2$	2	4	0.13
	$[\pi f_{7/2}, (\nu d_{5/2}, \nu g_{7/2}) 4] 11/2$	0	0	-0.11		$[\pi g_{9/2}, (\nu d_{5/2}, \nu g_{7/2}) 5] 19/2$	0	0	0.56
	$[\pi f_{7/2}, (\nu d_{5/2}, \nu g_{7/2}) 5] 13/2$	1	2	0.13		$[\pi g_{9/2}, (\nu d_{5/2}, \nu g_{7/2}) 5] 19/2$	1	2	-0.28
	$[\pi f_{7/2}, (\nu d_{5/2}, \nu g_{7/2}) 5] 15/2$	1	2	0.13		$[\pi g_{9/2}, (\nu d_{5/2}, \nu g_{7/2}) 5] 19/2$	2	0	0.18
	$[\pi g_{9/2}, (\nu g_{7/2}, \nu h_{11/2}) 7] 23/2$	1	2	0.12		$[\pi g_{9/2}, (\nu d_{5/2}, \nu g_{7/2}) 6] 19/2$	0	0	-0.26
	$[\pi g_{9/2}, (\nu g_{7/2}, \nu h_{11/2}) 9] 27/2$	0	0	-0.75		$[\pi g_{9/2}, (\nu d_{5/2}, \nu g_{7/2}) 6] 19/2$	1	2	0.17
	$[\pi g_{9/2}, (\nu g_{7/2}, \nu h_{11/2}) 9] 27/2$	1	2	0.57		$[\pi g_{9/2}, (\nu d_{5/2}, \nu g_{7/2}) 6] 21/2$	1	2	-0.30
	$[\pi g_{9/2}, (\nu g_{7/2}, \nu h_{11/2}) 9] 27/2$	2	0	-0.12		$[\pi g_{9/2}, (\nu d_{5/2}, \nu g_{7/2}) 6] 21/2$	2	4	0.13
	$[\pi g_{9/2}, (\nu g_{7/2}, \nu h_{11/2}) 9] 27/2$	2	2	0.13	$21/2_1^+$	$\pi g_{9/2}$	3	6	0.38
	$[\pi g_{9/2}, (\nu g_{7/2}, \nu h_{11/2}) 9] 27/2$	2	4	-0.18		$\pi g_{9/2}$	4	6	-0.13
$9/2_1^+$	$\pi g_{9/2}$	0	0	0.84		$[\pi g_{9/2}, (\nu d_{5/2}, \nu g_{7/2}) 4] 17/2$	1	2	-0.12
	$\pi g_{9/2}$	1	2	-0.49		$[\pi g_{9/2}, (\nu d_{5/2}, \nu g_{7/2}) 5] 17/2$	1	2	0.11
	$\pi g_{9/2}$	2	4	0.12		$[\pi g_{9/2}, (\nu d_{5/2}, \nu g_{7/2}) 5] 19/2$	1	2	-0.18
$5/2_1^+$	$\pi d_{5/2}$	0	0	0.10		$[\pi g_{9/2}, (\nu d_{5/2}, \nu g_{7/2}) 6] 21/2$	0	0	-0.24
	$\pi g_{9/2}$	1	2	0.80		$[\pi g_{9/2}, (\nu d_{5/2}, \nu g_{7/2}) 6] 21/2$	1	2	0.10
	$\pi g_{9/2}$	2	2	-0.52		$[\pi g_{9/2}, (\nu g_{7/2})^2 2] 13/2$	2	4	-0.12
	$\pi g_{9/2}$	3	3	0.15		$[\pi g_{9/2}, (\nu g_{7/2})^2 4] 17/2$	1	2	0.22
	$[\pi g_{9/2}, (\nu s_{1/2}, \nu d_{5/2}) 2] 5/2$	0	0	0.11		$[\pi g_{9/2}, (\nu g_{7/2})^2 6] 17/2$	1	2	0.10
$7/2_1^+$	$\pi g_{9/2}$	1	2	0.91		$[\pi g_{9/2}, (\nu g_{7/2})^2 6] 21/2$	0	0	-0.58
	$\pi g_{9/2}$	2	4	-0.30		$[\pi g_{9/2}, (\nu g_{7/2})^2 6] 21/2$	1	2	0.41
	$[\pi g_{9/2}, (\nu s_{1/2}, \nu d_{5/2}) 2] 7/2$	0	0	0.16		$[\pi g_{9/2}, (\nu g_{7/2})^2 6] 21/2$	2	0	-0.11
$11/2_1^+$	$\pi g_{9/2}$	1	2	0.79		$[\pi g_{9/2}, (\nu g_{7/2})^2 6] 21/2$	2	4	-0.12

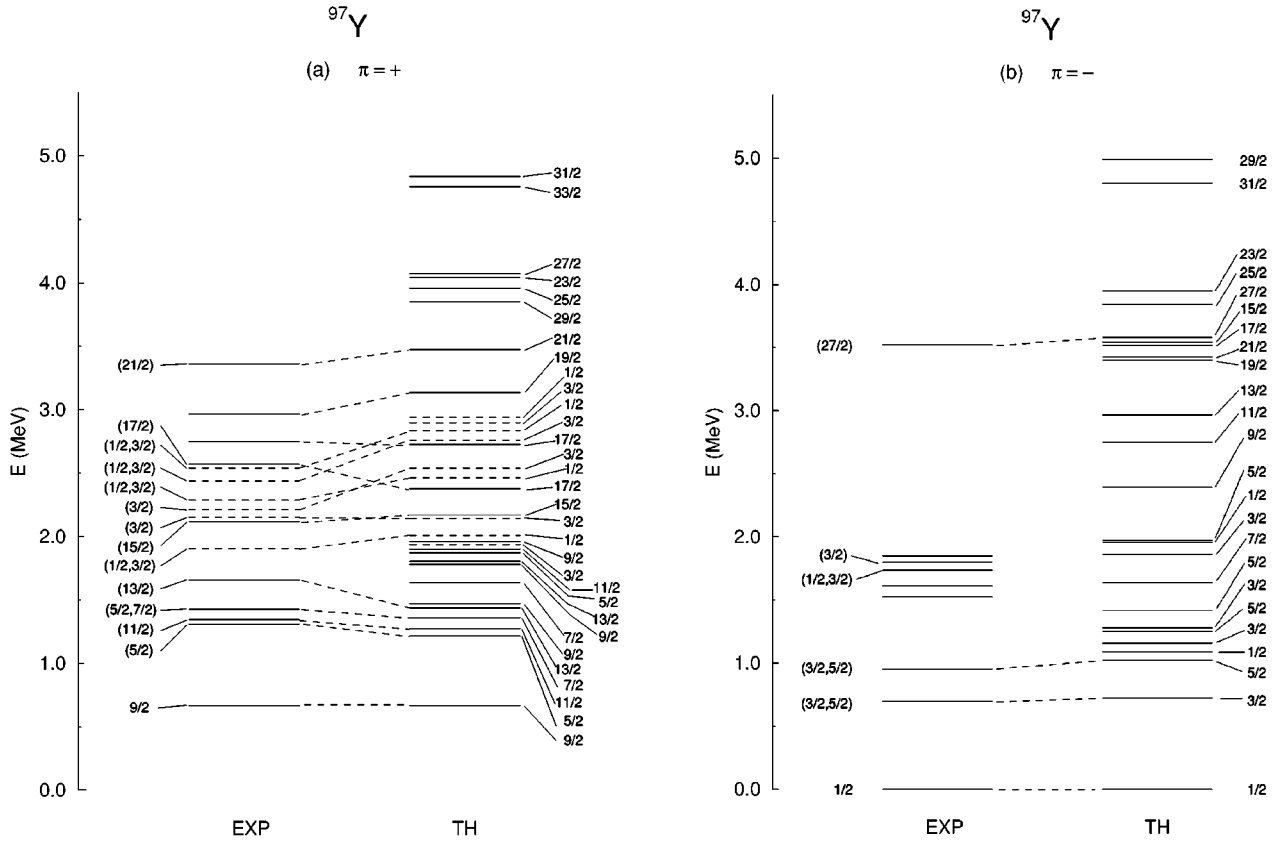


FIG. 1. Calculated states in  $^{97}\text{Y}$  of (a) positive parity and (b) negative parity in comparison to the available data. Above 2 MeV of excitation energy only the calculated yrast states are shown and, in the energy interval between 2 and 3 MeV the calculated  $1/2^+$  and  $3/2^+$  states (dashed lines). Calculated states are tentatively assigned to the experimental levels.

IBFBPM parameters for these two isotones. We found that the parameter values are mutually consistent. The main difference lies in quasiproton energies and occupation probabilities, reflecting the presence of two additional protons in  $^{99}\text{Nb}$ . Consequently, the  $\pi\tilde{g}_{9/2}$  quasiparticle in  $^{97}\text{Y}$  lies above  $\pi\tilde{p}_{1/2}$ , and in  $^{99}\text{Nb}$  below. The boson core parameters for  $^{99}\text{Nb}$  are similar to those used here for  $^{97}\text{Y}$ , with the boson parameter  $h1$  slightly shifted down from 0.815 MeV to 0.715 MeV. This shift is in qualitative accordance with an additional departure from the doubly-subshell closure in  $^{96}\text{Zr}$ . Furthermore, the monopole boson-fermion interaction term was increased from 0.02 MeV to 0.06 MeV, remaining small in magnitude. All other parameters have the same value in both nuclei, including the boson-fermion dynamical and exchange interactions. Thus, for the so far investigated  $^{97}\text{Y}$  and  $^{99}\text{Nb}$  isotones IBFBPM parameters appear mutually consistent.

### III. DISCUSSION

The calculated low-lying negative-parity triplet  $1/2_1^-$ ,  $3/2_1^-$ , and  $5/2_1^-$  is based on the one-quasiproton states  $\pi\tilde{p}_{1/2}$ ,  $\pi\tilde{p}_{3/2}$ , and  $\pi\tilde{f}_{5/2}$ , respectively. The admixtures of components containing three-quasiparticle states are very small:  $P_3(1/2_1^-) = 0.002$ ,  $P_3(3/2_1^-) = 0.008$ , and  $P_3(5/2_1^-) = 0.029$ , showing that these states have an approximate IBFM structure. Of similar character are the  $7/2_1^-$  and  $9/2_1^-$  states, hav-

ing  $|\pi\tilde{p}_{3/2}, 12; 7/2\rangle$  and  $|\pi\tilde{p}_{3/2}, 24; 9/2\rangle$  as the largest components. However, between the  $9/2_1^-$  and  $11/2_1^-$  calculated states there appears a band crossing: the  $11/2_1^-$  state, based on the three-quasiparticle state  $[\pi\tilde{p}_{1/2}, (\nu\tilde{d}_{5/2}, \nu\tilde{g}_{7/2})5]11/2^-$ , is lowered below the states based on components containing one-quasiparticle states. All the calculated higher-lying yrast states are based on components containing three-quasiparticle states.

Of particular interest is the  $27/2_1^-$  state having the  $[[\pi\tilde{g}_{9/2}, (\nu\tilde{g}_{7/2}, \nu\tilde{h}_{11/2})9]27/2^-]$  three-quasiparticle state as the largest component (56%), while the  $25/2_1^-$  and  $23/2_1^-$  states lie above it [see Fig. 1(b)]. Thus, the  $27/2_1^-$  state cannot decay by  $E2$  or  $M1$  transitions.

The calculated positive-parity states  $23/2_1^+$ ,  $25/2_1^+$ ,  $27/2_1^+$ ,  $29/2_1^+$ , and  $31/2_1^+$  also lie above the calculated  $27/2_1^-$  state [see Fig. 1(a)], and thus the  $27/2_1^-$  state cannot decay by  $E1$  or  $M2$  transitions either. On the other hand, the  $21/2_1^+$  state based on the  $[\pi\tilde{g}_{9/2}, (\nu\tilde{g}_{7/2})^26]21/2^+$  configuration is closely lying below the  $27/2_1^-$  state. Thus, the calculated  $27/2_1^-$  state is an isomer decaying by the  $E3$  transition to the close-lying  $21/2_1^+$  state. This is in accordance with the properties of the experimental 3523 keV ( $27/2^-$ ) isomer which only decays into the 3361 keV ( $21/2^+$ ) state [6] and to  $^{97}\text{Zr}$  by allowed Gamow-Teller  $\beta$  decay [29]. In Ref. [6] it was proposed that the most reasonable choices for the configurations of the 3523 keV isomer and of the 3361 keV level

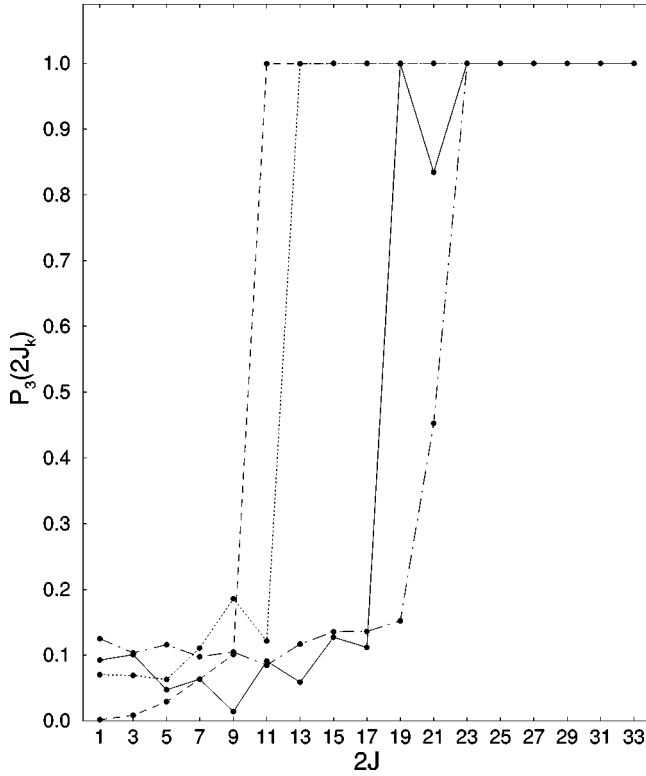


FIG. 2. Total weight of components containing three-quasiparticle states in the yrast and yrare states of positive and negative parity. Solid line: yrast states of positive parity; dashed line: yrast states of negative parity; dot-dashed line: yrare states of positive parity; dotted line: yrare states of negative parity.

are  $[[\pi g_{9/2}, (\nu g_{7/2}, \nu h_{11/2})9]27/2^-]$  and  $[[\pi g_{9/2}, (\nu d_{5/2}, \nu g_{7/2})6]21/2^+]$ , respectively. Depopulation of the 3523 keV isomer was thus attributed to the  $\nu h_{11/2} \rightarrow \nu d_{5/2}$   $E3$  transition. In the present IBFBPM calculation the main component in the  $27/2_1^-$  wave function is in accordance with the above prediction, while the  $21/2_1^+$  wave function contains two sizeable components with zero  $d$  bosons:  $[[\pi \tilde{g}_{9/2}, (\nu \tilde{g}_{7/2})^2 6]21/2, 00; 21/2^+]$  (34%) and  $[[\pi \tilde{g}_{9/2}, (\nu \tilde{d}_{5/2}, \tilde{g}_{7/2})6]21/2, 00; 21/2^+]$  (6%). However, because of reduction of the spin-flip matrix element  $\langle \tilde{g}_{7/2} || Y_3 || \tilde{h}_{11/2} \rangle$ , the leading contribution in IBFBPM too comes from the  $\nu \tilde{h}_{11/2} \rightarrow \nu \tilde{d}_{5/2}$   $E3$  transition, in accordance with the interpretation made in Ref. [6].

Furthermore, in Ref. [6] it was argued that the state based on  $[\pi \tilde{g}_{9/2}, (\nu \tilde{g}_{7/2}, \nu \tilde{h}_{11/2})8]25/2^-$  configuration should lie above the 3.523 MeV isomer. This is in accordance with the IBFBPM calculation (see Fig. 1), where the  $25/2_1^-$  state, having  $[[\pi \tilde{g}_{9/2}, (\nu \tilde{g}_{7/2}, \tilde{h}_{11/2})9]25/2, 00; 25/2^-]$  as the largest component (59%), lies 0.26 MeV above the calculated  $27/2_1^-$  isomeric state. Another interesting point is a remark in Ref. [6] stating that the small energy difference of 0.162 MeV between the  $(27/2_1^-)$  and  $(21/2_1^+)$  states of the proposed nature is remarkable, because one would expect an energy difference of the order of 1 MeV on the basis of properties of the core. Namely, in some other even-even nuclei in this mass region the  $9^-$  states exist at energies which are comparable to the excitation energy of the observed isomer in

TABLE II. Calculated  $E2$  and  $M1$  transitions between the positive-parity yrast states for  $^{97}\text{Y}$  in comparison to the available experimental branching ratios. The assignment of the  $7/2_1^+$  state, however, is questionable (see text).

$J_i \rightarrow J_f$ ( $\hbar$ ) ( $\hbar$ )	$B(E2)$ ( $e^2 b^2$ )	$B(M1)$ ( $\mu_N^2$ )	Expt.	$I_\gamma$ Theory
$5/2_1^+ \rightarrow 9/2_1^+$	0.109	–	100	100
$11/2_1^+ \rightarrow 9/2_1^+$	0.127	0.144	100	100
$7/2_1^+ \rightarrow 11/2_1^+$	0.001	–	–	0.0
$\rightarrow 5/2_1^+$	0.025	0.308	20	0.4
$\rightarrow 9/2_1^+$	0.057	0.224	100	100
$13/2_1^+ \rightarrow 11/2_1^+$	0.014	0.197	37	10
$\rightarrow 9/2_1^+$	0.103	–	100	100
$15/2_1^+ \rightarrow 13/2_1^+$	0.056	0.087	–	50
$\rightarrow 11/2_1^+$	0.092	–	100	100
$17/2_1^+ \rightarrow 15/2_1^+$	0.017	0.250	6	36
$\rightarrow 13/2_1^+$	0.150	–	100	100
$17/2_2^+ \rightarrow 17/2_1^+$	0.031	0.002	58	0.1
$\rightarrow 15/2_1^+$	0.044	0.124	100	100
$\rightarrow 13/2_1^+$	0.001	–	–	2
$19/2_1^+ \rightarrow 17/2_2^+$	0.000	0.0001	53	1
$\rightarrow 17/2_1^+$	0.000	0.002	100	100
$\rightarrow 15/2_1^+$	0.0001	–	–	32
$21/2_1^+ \rightarrow 19/2_1^+$	0.013	0.184	19	172
$\rightarrow 17/2_2^+$	0.001	–	9	1
$\rightarrow 17/2_1^+$	0.031	–	100	100

$^{97}\text{Y}$ . Thus, bands in Pd isotopes are based on  $9^-$  levels [30] which were interpreted in terms of the  $(\nu g_{7/2}, \nu h_{11/2})9^-$  configuration. In these cases, the energy difference between the  $6^+$  and  $9^-$  levels is of the order of 1 MeV. The experimental  $9^- - 6^+$  energy differences in  $^{96}\text{Sr}$  and  $^{98}\text{Zr}$ , the even-even neighboring isotones of  $^{97}\text{Y}$ , are unknown, but it was pointed out [6] that the values of 2.58 and 0.96 MeV [31] for the  $1h_{11/2} - 3s_{1/2}$  and  $2d_{5/2} - 3s_{1/2}$  single-particle energies, respectively, in  $^{97}\text{Zr}$  and  $^{95}\text{Zr}$  make it improbable that these states are very close. It was concluded therefore, that a rather strongly attractive interaction between the  $\pi g_{9/2}$  proton and the neutrons in the  $9^-$  broken pair should be present in  $^{97}\text{Y}$ . The present IBFBPM calculation gives a small energy splitting between the  $27/2_1^-$  and  $21/2_1^+$  states (0.11 MeV), in accordance with the experimental value.

The calculation also predicts the possible existence of yet another isomer below the  $27/2_1^-$  state. Namely, the  $17/2_1^-$  and  $15/2_1^-$  states lie above the close-lying doublet of  $19/2_1^-$  and  $21/2_1^-$  states. Thus, the calculated  $19/2_1^-$  and  $21/2_1^-$  states cannot decay by  $E2$  or  $M1$  transitions. Nevertheless, they might decay via a hindered  $E1$  transition to the lower-lying  $19/2_1^+$  and  $17/2_1^+$  positive-parity states.

Finally, let us comment in some details on the positive parity states calculated in IBFBPM. As seen from Fig. 1(a), we obtain the  $\Delta J=1$  positive-parity band  $9/2_1^+$ ,  $11/2_1^+$ ,  $13/2_1^+$ ,  $15/2_1^+$ ,  $17/2_1^+$ ,  $19/2_1^+$ ,  $21/2_1^+$ . The first five states are based on the configurations  $|\pi \tilde{g}_{9/2}, 00; 9/2\rangle$ ,  $|\pi \tilde{g}_{9/2}, 12; 11/2\rangle$ ,  $|\pi \tilde{g}_{9/2}, 12; 13/2\rangle$ ,  $|\pi \tilde{g}_{9/2}, 24; 15/2\rangle$ , and

$|\pi\tilde{g}_{9/2}, 24; 17/2\rangle$ , respectively, bearing a characteristic of the SU(5) (i.e., quasivibrational) pattern. The states  $19/2_1^+$  and  $21/2_1^+$  are based on the  $[[\pi\tilde{g}_{9/2}, (\nu\tilde{d}_{5/2}, \nu\tilde{g}_{7/2})5] 19/2, 00; 19/2]$  and  $[[\pi\tilde{g}_{9/2}, (\nu\tilde{g}_{7/2})^2 6] 21/2, 00; 21/2]$  three-quasiparticle components, respectively. Although the ordering of levels up to  $21/2_1^+$  is the normal one ( $\Delta J=1$ ), the branching ratios look characteristic of the multiplets associated with the SU(5) boson core. Namely, the  $11/2_1^+$  and  $13/2_1^+$  state arise in leading order from one- $d$ -boson multiplet, and thus in the leading order the  $13/2_1^+ \rightarrow 11/2_1^+$   $E2$  transition is of a  $\Delta n_d=0$  type and therefore hindered, while the  $13/2_1^+ \rightarrow 9/2_1^+$   $E2$  transition is of the  $\Delta n_d=1$  type and therefore allowed. In accordance with this leading order prediction, the calculated  $B(E2)$  ( $13/2_1^+ \rightarrow 9/2_1^+$ ) value is sizeably larger than  $B(E2)$  ( $13/2_1^+ \rightarrow 11/2_1^+$ ) and therefore the strongest branch depopulating the  $13/2_1^+$  state is  $13/2_1^+ \rightarrow 9/2_1^+$ , in accordance with experiment. A similar situation appears for the  $15/2_1^+$  and  $17/2_1^+$  states which arise in the leading order from a two- $d$ -boson multiplet, and consequently the strongest branch depopulating the  $17/2_1^+$  state is  $17/2_1^+ \rightarrow 13/2_1^+$  being of  $\Delta n_d=1$  type in the leading order. For the same reason, the main branch depopulating the  $15/2_1^+$  state is  $15/2_1^+ \rightarrow 11/2_1^+$ . However, the change of pattern appears for decay of  $19/2_1^+$  state containing a three-quasiparticle state in the dominant component. In our calculation this leads to a sizeable hindrance of the  $E2$  and  $M1$  transitions depopulating this level, but because of the  $M1$  contribution the  $19/2_1^+ \rightarrow 17/2_1^+$  transition is stronger than the  $19/2_1^+ \rightarrow 15/2_1^+$ . Sizable reduction of transitions depopulating the calculated  $19/2_1^+$  is a consequence of relatively small mixing of one- and three-quasiparticle components. If, however, the experimental  $E2$  decay of this state turns out to be stronger than predicted here, this would point out to a shortcoming of our parametrization and/or the influence of more complex terms in the interaction. In any case, the change of predominant  $\Delta J=2$  branch for depopulation of the states with  $J_1^+ \leq \frac{17}{2}_1^+$  into the  $\Delta J=1$  branch for depopulation of  $J_1^+ = \frac{19}{2}_1^+$  may be attributed to the onset of more important role of three-quasiparticle states in the  $19/2_1^+$  wave function. As to the decay pattern of the  $21/2_1^+$  state, both the  $21/2_1^+ \rightarrow 19/2_1^+$  and  $21/2_1^+ \rightarrow 17/2_1^+$  branching ratios are comparable (the first transition is even stronger), while experimentally the  $21/2_1^+ \rightarrow 19/2_1^+$  transition is five times weaker than the  $21/2_1^+ \rightarrow 17/2_1^+$ . This discrepancy indicates that the calculated  $B(M1)$  ( $21/2_1^+ \rightarrow 19/2_1^+$ ) value is by almost an order of magnitude too large. This might indicate that the  $\pi\tilde{g}_{9/2}$   $\nu\tilde{d}_{5/2}$   $\nu\tilde{g}_{7/2}$  components in the  $19/2_1^+$  and/or  $21/2_1^+$  states are too large.

Above the  $21/2_1^+$  state the normal-type band structure terminates: the next higher-lying yrast state is  $29/2_1^+$ , which is based on the  $[[\pi\tilde{g}_{9/2}, (\nu\tilde{h}_{11/2})^2 10] 29/2^+]$  three-quasiparticle configuration. This calculated state decays by  $E1$  transition into the  $27/2_1^-$  state. This transition proceeds via small admixtures in the wave function containing the  $\nu\tilde{g}_{9/2}$  or  $\nu\tilde{h}_{9/2}$  configurations from the shells below or above the valence shell, enabling the  $\nu\tilde{h}_{11/2} \rightarrow \nu\tilde{g}_{9/2}$  or  $\nu\tilde{h}_{9/2} \rightarrow \nu\tilde{g}_{7/2}$   $E1$  transitions. Consequently, this transition may be highly hindered.

Above the  $29/2_1^+$  state there appears a triplet of close-lying states  $25/2_1^+$ ,  $23/2_1^+$ , and  $27/2_1^+$ , which are based on the  $[[\pi\tilde{g}_{9/2}, (\nu\tilde{h}_{11/2})^2 8] 25/2^+]$ ,  $[[\pi\tilde{g}_{9/2}, (\nu\tilde{h}_{11/2})^2 8] 23/2^+]$ , and  $[[\pi\tilde{g}_{9/2}, (\nu\tilde{h}_{11/2})^2 10] 27/2^+]$  three-quasiparticle configurations, respectively.

Let us now discuss the  $1/2^+$  and  $3/2^+$  states in the energy interval between 1.8 and 3.0 MeV. Our calculation gives nine states [four  $1/2^+$  and five  $3/2^+$ ; see Fig. 1(a)], which is in rather good agreement with six experimentally  $1/2^+$ ,  $3/2^+$  states observed by  $\beta$  decay of  $I^\pi=1/2^+$   $^{97}\text{Sr}$  [32]. The weights of components containing the three-quasiparticle states are  $P_3(3/2_1^+)=0.101$ ,  $P_3(1/2_1^+)=0.093$ ,  $P_3(3/2_2^+)=0.103$ ,  $P_3(3/2_3^+)=0.126$ ,  $P_3(1/2_2^+)=0.125$ ,  $P_3(3/2_4^+)=0.132$ , and  $P_3(1/2_3^+)=0.134$ . Although the components containing one-quasiparticle states are dominant, the components containing three quasiparticles have an essential influence in compressing these group of low-lying  $1/2^+$ ,  $3/2^+$  levels.

We note that the theoretical assignments of levels shown in Fig. 1 and Table II are based on the presently available experimental data [33]. However, the 1428 keV level which was discussed as being the  $7/2^+$  member of the  $2^+ \otimes g_{9/2}$  multiplet [34], is a very probable  $5/2^+$  state according to our new data [35]. Thus, the theoretical  $7/2_1^+$  level was not observed. Furthermore, the experimental level at 1738 keV (not presented in Fig. 1) is probably  $3/2$  with either parity, and could be associated with the  $3/2_1^+$  theoretical level that we have not assigned to any known experimental level. Calculations in IBFBPM for  $^{99}\text{Nb}$  and correspondence to  $^{97}\text{Y}$  strongly support a  $3/2_1^+$  assignment, but the experimental evidence is rather speculative.

#### IV. CONCLUSION

The present calculation of the nuclear structure of the transitional nucleus  $^{97}\text{Y}$  reveals an interplay of one- and three-quasiparticle states in the framework of the interacting boson fermion model. In particular, we obtain theoretically a band crossing between the  $9/2_1^-$  and  $11/2_1^-$  states for the configurations based on components containing one-quasiproton to the configurations based on components containing one-quasiproton-two-quasineutron components. Simultaneously, the present calculation predicts the  $27/2_1^-$  isomeric state decaying predominantly by  $E3$  transition into the  $21/2_1^+$  state, in accordance with experiment. The calculation also reproduces a small energy splitting between the  $27/2_1^-$  and  $21/2_1^+$  states. The general agreement between the present IBFBPM calculation and experiment is reasonable. It is also interesting to compare the structure of the isotones  $^{97}\text{Y}$  and  $^{99}\text{Nb}$ . Detailed comparison of  $^{97}\text{Y}$  and  $^{99}\text{Nb}$  levels will be published along with new experimental data for  $^{99}\text{Nb}$  [35].

#### ACKNOWLEDGMENT

Part of this work was supported by the Academy of Finland.

- [1] G. Lhersonneau, B. Pfeiffer, K.-L. Kratz, T. Enqvist, P. P. Jauho, A. Jokinen, J. Kantele, M. Leino, J. M. Parmonen, H. Penttilä, J. Äystö, and the ISOLDE Collaboration, *Phys. Rev. C* **49**, 1379 (1994).
- [2] M. L. Stolzenwald, S. Brant, H. Ohm, K. Sistemich, and G. Lhersonneau, in *Proceedings of Nuclear Structure of the Zirconium Region*, edited by J. Eberth, R. A. Meyer, and K. Sistemich (Springer, Berlin, 1988).
- [3] R. A. Meyer, E. Monnard, J. A. Pinston, F. Schussler, I. Ragnarsson, B. Pfeiffer, H. Lawin, G. Lhersonneau, T. Seo, and K. Sistemich, *Nucl. Phys.* **A439**, 510 (1985).
- [4] K. Sistemich, G. Sadler, T. A. Khan, J. W. Gräter, W. D. Lauppe, H. Lawin, H. A. Selič, F. Schussler, J. Blachot, J. P. Bocquet, E. Monnard, and B. Pfeiffer, *Proceedings of the 3rd International Conference on Nuclei far from Stability*, Cargèse, 1976 [Report CERN 76-13, 495 (1977)].
- [5] E. Monnard, J. Blachot, F. Schussler, J. P. Bocquet, B. Pfeiffer, G. Sadler, H. A. Selič, T. A. Khan, W. D. Lauppe, H. Lawin, and K. Sistemich, *Proceedings of the 3rd International Conference on Nuclei far from Stability*, Cargèse, 1976 [Report CERN 76-13, 477 (1977)].
- [6] G. Lhersonneau, D. Weiler, P. Kohl, H. Ohm, and K. Sistemich, *Z. Phys. A* **323**, 59 (1986).
- [7] G. Lhersonneau *et al.*, *Nucl. Instrum. Methods Phys. Res. A* **373**, 415 (1996).
- [8] S. Brant, K. Sistemich, V. Paar, and G. Lhersonneau, *Z. Phys. A* **330**, 365 (1988).
- [9] D. Vretenar, G. Bonsignori, and M. Savoia, *Z. Phys. A* **351**, 289 (1995).
- [10] C. Rossi Alvarez, D. Vretenar, Zs. Podolyák, D. Bazzacco, G. Bonsignori, F. Brandolini, S. Brant, G. de Angelis, M. De Poli, M. Ionescu-Bujor, Y. Li, S. Lunardi, N. H. Medina, and C. M. Petrache, *Phys. Rev. C* **54**, 57 (1996).
- [11] C. M. Petrache, R. Venturelli, D. Vretenar, D. Bazzacco, G. Bonsignori, S. Brant, S. Lunardi, M. A. Rizzutto, C. Rossi Alvarez, G. de Angelis, M. De Poli, and D. R. Napoli, *Nucl. Phys.* **A617**, 228 (1997).
- [12] F. Iachello and A. Arima, *The Interacting Boson Model* (Cambridge University Press, Cambridge, England, 1987).
- [13] A. Arima and F. Iachello, *Phys. Rev. Lett.* **35**, 157 (1975); *Ann. Phys. (N.Y.)* **99**, 233 (1976); **111**, 201 (1978); **123**, 468 (1979).
- [14] F. Iachello and O. Scholten, *Phys. Rev. Lett.* **43**, 679 (1979).
- [15] F. Iachello and P. Van Isacker, *The Interacting Boson Fermion Model* (Cambridge University Press, Cambridge, England, 1991).
- [16] O. Scholten, *Prog. Part. Nucl. Phys.* **14**, 189 (1985).
- [17] V. Paar, in *Capture Gamma-ray Spectroscopy and Related Topics*, AIP Conf. Proc. No. 125, edited by S. Raman (AIP, New York, 1985), p. 70.
- [18] S. Brant, V. Paar, and D. Vretenar, *Z. Phys. A* **319**, 355 (1984); V. Paar, D. K. Sunko, and D. Vretenar, *ibid.* **327**, 291 (1987).
- [19] F. Iachello and D. Vretenar, *Phys. Rev. C* **43**, 945 (1991).
- [20] D. Vretenar, V. Paar, G. Bonsignori, and M. Savoia, *Phys. Rev. C* **42**, 993 (1990); **44**, 223 (1991).
- [21] D. Vretenar, G. Bonsignori, and M. Savoia, *Phys. Rev. C* **47**, 2019 (1993).
- [22] C. J. Lister, P. Chowdhury, and D. Vretenar, *Nucl. Phys.* **A557**, 361 (1993).
- [23] J. Timár, T. X. Quang, T. Fényes, Zs. Dombrádi, A. Krasznahorkay, J. Kumpulainen, R. Julin, S. Brant, V. Paar, and Lj. Šimičić, *Nucl. Phys.* **A573**, 61 (1994).
- [24] S. Brant, V. Paar, G. Lhersonneau, O. W. B. Schult, H. Seyfarth, and K. Sistemich, *Z. Phys. A* **334**, 517 (1989).
- [25] L. S. Kisslinger and R. A. Sorensen, *Rev. Mod. Phys.* **35**, 853 (1963).
- [26] G. Lhersonneau, S. Brant, H. Ohm, V. Paar, K. Sistemich, and D. Weiler, *Z. Phys. A* **334**, 259 (1989).
- [27] G. de Angelis, M. A. Cardona, M. de Poli, S. Lunardi, D. Bazzacco, F. Brandolini, D. Vretenar, G. Bonsignori, M. Savoia, and R. Wyss, *Phys. Rev. C* **49**, 2990 (1994).
- [28] D. Sohler *et al.*, *Z. Phys. A* **357**, 239 (1997).
- [29] G. Lhersonneau, P. Dendooven, S. Hankonen, A. Honkanen, M. Huhta, R. Julin, S. Juutinen, M. Oinonen, H. Penttilä, A. Savelius, S. Törmänen, and J. Äystö, *Phys. Rev. C* **54**, 1117 (1996).
- [30] J. A. Grau, L. E. Samuelson, P. A. Rickey, P. C. Simms, and G. J. Smith, *Phys. Rev. C* **14**, 2297 (1976).
- [31] C. R. Bingham and G. T. Fabian, *Phys. Rev. C* **7**, 150 (1973).
- [32] B. Pfeiffer, E. Monnard, J.A. Pinston, F. Schussler, C. Jung, J. Münzel, and H. Wollnik, in *Proceedings of the International Conference on Nuclei far from Stability*, Helsingor, Denmark [Report CERN 81-89, 1981], Vol. 2, p. 423.
- [33] A. Artua-Cohen, *Nucl. Data Sheets* **70**, 85 (1993).
- [34] M. Büscher, R. F. Casten, R. L. Gill, R. Schuhmann, J. A. Winger, H. Mach, M. Moszyński, and K. Sistemich, *Phys. Rev. C* **41**, 1115 (1990).
- [35] G. Lhersonneau *et al.* (unpublished).